SCIENCE CHINA
Information Sciences

• RESEARCH PAPER •

January 2020, Vol. 63 112206:1–112206:13
https://doi.org/10.1007/s11432-018-9933-6

Improving dynamics of integer-order small-world network models under fractional-order PD control

Huaifei WANG[1], Min XIAO[1,2*], Binbin TAO[1], Fengyu XU[1], Zhengxin WANG[3], Chengdai HUANG[4] & Jianlong QIU[5]

[1]*College of Automation, Nanjing University of Posts and Telecommunications, Nanjing* 210003*, China;*
[2]*School of Mathematics and Physics, Qingdao University of Science and Technology, Qingdao* 266061*, China;*
[3]*College of Science, Nanjing University of Posts and Telecommunications, Nanjing* 210003*, China;*
[4]*School of Mathematics and Statistics, Xinyang Normal University, Xinyang* 464000*,China;*
[5]*School of Automation and Electrical Engineering, Linyi University, Linyi* 276005*, China*

Received 7 November 2018/Revised 1 May 2019/Accepted 30 May 2019/Published online 25 December 2019

Abstract The optimal control of dynamics is a popular topic for small-world networks. In this paper, we address the problem of improving the behavior of Hopf bifurcations in an integer-order model of small-world networks. In this study, the time delay is used as the bifurcation parameter. We add a fractional-order proportional-derivative (PD) scheme to an integer-order Newman-Watts (N-W) small-world model to better control the Hopf bifurcation of the model. The most important contribution of this paper involves obtaining the stability of the system and the variation of the conditions of the Hopf bifurcation after a fractional PD controller is added to the integer-order small-world model. The results demonstrate that the designed PD controller can be used to restrain or promote the occurrence of Hopf bifurcations by setting appropriate parameters. We also describe several simulations to verify our research results.

Keywords small-world networks, stability, Hopf bifurcation, bifurcation control, fractional-order PD control

Citation Wang H F, Xiao M, Tao B B, et al. Improving dynamics of integer-order small-world network models under fractional-order PD control. Sci China Inf Sci, 2020, 63(1): 112206, https://doi.org/10.1007/s11432-018-9933-6

1 Introduction

A simple network called a small-world network was developed in 1998 [1]. This network can describe the gradual process from a rule lattice to a random graph. Many common problems pertaining to small-world networks have been demonstrated through various studies. The model is linear and simplified as the reaction instantaneous network, and the communication delay is ignored. In the present study, we only consider the influence of time delay and nonlinear topology on the model, and ignore the topological differences of the nonlinear constant interaction in the model [2,3]. The study of the common Newman-Watts (N-W) model is a popular topic in Hopf bifurcation research.

In recent years, increasing attention has been paid to the dynamic characteristics of small-world networks [3–14]. Recent studies on small-world network are plentiful, addressing not only sensitivity and stability, but also periodic oscillatory behavior, chaos, and bifurcation [15,16]. For example, Xu et al. [5] investigated the dynamic control of a small-world network with memory, and Mahajan et al. [9] discussed the transition from clustered states to spatiotemporal chaos in small-world networks. Maslennikov et al. [11] studied the basin stability for burst synchronization in small-world networks of chaotic slow-fast oscillators.

* Corresponding author (email: candymanxm2003@aliyun.com)

A Hopf bifurcation is a strategy for handling various dynamic properties of nonlinear systems, ranging from the equilibrium point, periodic oscillation, and chaos [17–20]. More detailed information about the performance of periodic solutions around the equilibrium can be derived following specific Hopf bifurcation analysis. In recent years, there has been much progress in Hopf bifurcation research for small-world networks. Xiao et al. [13] addressed the control of Hopf bifurcations of the fractional-order small-world network model, while Zhou et al. [14] investigated the stability, instability, and Hopf bifurcation of a delayed small-world network model with excitatory or inhibitory short-cuts.

Control strategy is a common method for improving the performance of complex networks. With the development of complex networks, an increasing number of control strategies are in use, such as adaptive control [21], state feedback control [22], impulsive control [23], robust disturbance rejection control [24], and fault-tolerant control [25]. Control strategy has been successfully applied in complex network systems of integer order and achieved the aim of control. However, a number of shortcomings remain. To compensate for these shortcomings, a practical controller called a proportional-derivative (PD) feedback controller is introduced to control the Hopf bifurcation arising in complex networks [13,26,27]. Compared with state feedback control (or delayed feedback control), the PD scheme can greatly simplify the analysis when the system contains only delay terms. In contrast to hybrid controller, the PD controller has two adjustable parameters, making the design more flexible. In addition, the design of the PD controller is more convenient and affordable than that of fault-tolerant control technology. The purpose of bifurcation control can be achieved under only a small control force as it tends to vanish once stabilization is achieved. For these reasons, the PD controllers have been widely investigated in recent years.

Researchers in the control community have applied PD control schemes to interfere with the performance of researched systems and models. PD control has been extensively applied in robotic manipulation. For example, Zhang et al. [28] investigated switched fuzzy-PD control of contact forces in robotic microbio manipulation. In addition, position domain nonlinear PD control for contour tracking of robotic manipulators was proposed in [29]. Furthermore, complex networks under PD controllers have been widely investigated in recent years. Ding et al. [26] controlled the intrinsic occurrence of a Hopf bifurcation in an N-W network model by adding a PD controller, while Tang et al. [27] applied a designed PD control to a congestion control system. Xiao et al. [13] addressed the problem of fractional-order PD control in small-world networks and demonstrated that the onset of Hopf bifurcations can be altered via the proposed PD controller by setting proper control parameters. Özbay et al. [30] studied PID controller design for fractional-order systems with time delay. In this paper, we focus on fractional-order PD control of an N-W small-world network and further examine the stability, bifurcation and periodic solution of the controlled network.

In exiting studies, the order of the small-world network model is the same as that of the derivative term in the PD controller [13, 27], which fails to generalize the controlled model to a further extent. Unlike previous studies, our aim in this study is to apply a PD controller with variable order in the derivation term to an integer-order small-world network with time delay. It should be noted that the order of the small-world network model is inconsistent with that of the derivative in a PD controller. The fractional-order PD control proposed in this paper is therefore more general.

The contributions of this paper are four-fold:

(1) A fractional-order PD controller with variable order is used to interfere with the dynamics of an integer-order small-world network model, and the variable order of the fractional derivative is taken proportionally as $\frac{1}{n}$ in the control process.

(2) The order of the PD controller differs from that of the small-world network model. We apply a fractional-order PD controller to an integer-order small-world network model, thus extending the variety of controllable systems.

(3) The initiation of the inherent Hopf bifurcation can be effectively delayed or advanced by setting appropriate proportional and derivative control parameters. Thus, dynamical behaviors of small-world networks can be optimized under fractional-order PD control.

(4) The designed fractional-order PD control scheme can also be applied to bifurcation control of general integer-order systems with time delay. The control scheme proposed in this paper serves to

provide a reference for bifurcation control of integer-order delayed systems.

The remainder of this paper is structured as follows. In Section 2, we introduce the Caputo derivative and an integer-order small-world network model with time delay. In Section 3, by analyzing the stability, we obtain the bifurcation conditions of the system. In Section 4, we present several numerical simulations to support the theoretical outcomes. In Section 5, we conclude the paper.

2 Preliminaries

As a general rule, we have used three common fractions in previous research: the Grunwald-Letnikov fractional derivative, the Caputo fractional derivative, and the Riemann-Liouville fractional derivative [31–34]. Because the Caputo fractional derivative has the advantage of not limiting the initial conditions of the system, it is more suitable for practical engineering problems [35, 36]. The main fractional order used in this paper is the Caputo derivative, which is defined as follows.

Definition 1 ([37]). The Caputo fractional derivative can be expressed as

$$ {}_0^C D_t^{\varpi} f(t) = \frac{1}{\varsigma(\varphi - \varpi)} \int_0^t (t-\tau)^{\varphi-\varpi-1} f^{(\varphi)}(\tau) \mathrm{d}\tau, \tag{1} $$

where $\varpi \geqslant 0$, $\varphi - 1 \leqslant \varpi < \varphi$ and $\varphi \in Z^+$. Here, $\varsigma(\cdot)$ is the Gamma function and $\varsigma(s) = \int_0^{+\infty} t^{s-1} \mathrm{e}^{-t} \mathrm{d}t$. In addition, ϖ indicates the value of the fraction-order that is normally selected in range $\varpi \in (0, 1)$.

Theorem 1 ([38]). The semi-group property of the fractional-order differential can be described as: If $f(t) \in C[0, \kappa]$, $\kappa > 0$, $\alpha \in R^+$, $\beta \in R^+$ and $\alpha + \beta \leqslant 1$ hold, then

$$ {}_0^C D_t^{\alpha} {}_0^C D_t^{\beta} f(t) = {}_0^C D_t^{\beta} {}_0^C D_t^{\alpha} f(t) = {}_0^C D_t^{\alpha+\beta} f(t), \quad t \in [0, \kappa]. $$

Model description. The N-W network model was proposed to explain the spread of diseases [2]. However, this model has shortcomings; for instance, it omits transmission delay. In this study, we examine a small-world model with the interference of time delays and nonlinear couplings. The model can be described as follows:

$$ \dot{i}(t) = \varepsilon + i(t-\tau) - \mu\varepsilon i^2(t-\tau), \tag{2} $$

where $i(t)$ is the total impact volume, τ is the time delay, and μ and ε are the measures of nonlinear interactions and the length scale, respectively.

Let i^* be an equilibrium point of model (2). Then, Eq. (2) becomes

$$ \varepsilon + i^* - \mu\varepsilon(i^*)^2 = 0. \tag{3} $$

By solving (3), it is simple to obtain a positive equilibrium point $i^* = \frac{1+\sqrt{1+4\mu\varepsilon^2}}{2\mu\varepsilon}$.

3 Hopf bifurcation control via PD$^{1/n}$ feedback controller

In this section, we present the design of a PD controller for model (2) to regulate the occurrence of a Hopf bifurcation. An ordinary PD controller is expressed as follows:

$$ u(t) = K_p[i(t) - i^*] + K_d \left[{}_0^C D_t^{\frac{1}{n}} (i(t) - i^*) \right], \tag{4} $$

where K_p and K_d represent the proportional gain and derivation gain, respectively.

Remark 1. If $n = 1$, Eq. (4) is a traditional PD controller. If $n \geqslant 2$, Eq. (4) is a fractional PD controller. Therefore, Eq. (4) is a generalization of the traditional PD controller.

Thus, we can obtain a controlled fractional-order small-world network model via the designed PD controller (4) as follows:

$$\dot{i}(t) = \varepsilon + i(t-\tau) - \mu\varepsilon i^2(t-\tau) + K_p[i(t) - i^*] + K_d\left[{}_0^C D_t^{\frac{1}{n}}(i(t) - i^*)\right]. \tag{5}$$

Let

$$\begin{aligned} l_1(t) &= i(t) - i^*, \\ l_2(t) &= {}_0^C D_t^{\frac{1}{n}} l_1(t), \\ l_3(t) &= {}_0^C D_t^{\frac{1}{n}} l_2(t), \\ &\vdots \\ l_n(t) &= {}_0^C D_t^{\frac{1}{n}} l_{n-1}(t). \end{aligned} \tag{6}$$

From Theorem 1, we have

$$\begin{aligned} &{}_0^C D_t^{\frac{1}{n}} l_n(t) \\ &= {}_0^C D_t^{\frac{1}{n}}\left[{}_0^C D_t^{\frac{1}{n}} l_{n-1}(t)\right] \\ &= {}_0^C D_t^{\frac{2}{n}} l_{n-1}(t) = \cdots = {}_0^C D_t^{\frac{n}{n}} l_1(t) = \dot{l}_1(t) = \dot{i}(t) \\ &= \varepsilon + l_1(t-\tau) + i^* - \mu\varepsilon(l_1(t-\tau) + i^*)^2 + K_p l_1(t) + K_d l_2(t). \end{aligned}$$

Therefore, the controlled N-W model (5) is equivalent to the following n-dimensional system:

$$\begin{aligned} &{}_0^C D_t^{\frac{1}{n}} l_1(t) = l_2(t), \\ &{}_0^C D_t^{\frac{1}{n}} l_2(t) = l_3(t), \\ &\quad\vdots \\ &{}_0^C D_t^{\frac{1}{n}} l_{n-1}(t) = l_n(t), \\ &{}_0^C D_t^{\frac{1}{n}} l_n(t) = \varepsilon + l_1(t-\tau) + i^* - \mu\varepsilon(l_1(t-\tau) + i^*)^2 + K_p l_1(t) + K_d l_2(t). \end{aligned} \tag{7}$$

The linearized model of the controlled N-W model (5) at the equilibrium point can be represented as follows:

$$\begin{aligned} &{}_0^C D_t^{\frac{1}{n}} l_1(t) = l_2(t), \\ &{}_0^C D_t^{\frac{1}{n}} l_2(t) = l_3(t), \\ &\quad\vdots \\ &{}_0^C D_t^{\frac{1}{n}} l_{n-1}(t) = l_n(t), \\ &{}_0^C D_t^{\frac{1}{n}} l_n(t) = (1 - 2\mu\varepsilon i^*) l_1(t-\tau) + K_p l_1(t) + K_d l_2(t). \end{aligned} \tag{8}$$

The following features can be obtained by sorting (8):

$$\left|S^{\frac{1}{n}} - A\right| = \det\begin{bmatrix} S^{\frac{1}{n}} & -1 & 0 & \cdots & 0 \\ 0 & S^{\frac{1}{n}} & -1 & \cdots & 0 \\ \vdots & \vdots & \vdots & & \vdots \\ 0 & 0 & 0 & \cdots & -1 \\ -(1 - 2\mu\varepsilon V^*)\mathrm{e}^{-S\tau} - K_p & -K_d & 0 & \cdots & S^{\frac{1}{n}} \end{bmatrix} = 0. \tag{9}$$

Thus,

$$S - K_d S^{\frac{1}{n}} - a\mathrm{e}^{-S\tau} - K_p = 0, \tag{10}$$

where

$$a = 1 - 2\mu\varepsilon i^* = -\sqrt{1 + 4\mu\varepsilon^2} < 0.$$

3.1 Case without delays ($\tau = 0$)

When $\tau = 0$, Eq. (10) becomes

$$S - K_d S^{\frac{1}{n}} - a - K_p = 0. \tag{11}$$

Lemma 1. If $K_p < -a$ and $K_d < 0$, the roots of (11) must have negative real parts.

Proof. Let $S = A\mathrm{e}^{\mathrm{i}\theta} = A(\cos\theta + \mathrm{i}\sin\theta)$. A is the modulus and θ is the argument of S on the complex plane. Therefore, Eq. (11) can be equally expressed as

$$A(\cos\theta + \mathrm{i}\sin\theta) - K_d A^{\frac{1}{n}} \left(\cos\frac{\theta}{n} + \mathrm{i}\sin\frac{\theta}{n}\right) - a - K_p = 0. \tag{12}$$

Eq. (12) then becomes the following equation by separating the real and imaginary parts:

$$\begin{cases} A\cos\theta - K_d A^{\frac{1}{n}} \cos\dfrac{\theta}{n} - a - K_p = 0, \\ A\sin\theta - K_d A^{\frac{1}{n}} \sin\dfrac{\theta}{n} = 0. \end{cases} \tag{13}$$

It is clear that, when $K_p < -a$, $K_d < 0$ and $\theta \in [-\frac{\pi}{2}, \frac{\pi}{2}]$, Eq. (13) has no roots with positive real parts. As a result, the roots of (11) must have negative real parts. This ends the proof.

Theorem 2. If $K_p < -a$ and $K_d < 0$, the controlled model (5) with n ($n \in Z^+$) and $\tau = 0$ is asymptotically stable at the equilibrium point.

Remark 2. When $n = 1$, the fractional-order PD controller (4) degenerates to an integer-order PD controller, and (11) has a negative root $S = \frac{a+K_p}{1-K_d}$ if $K_p < -a$ and $K_d < 1$. Thus, we can conclude that the controlled model (5) with $n = 1$ and $\tau = 0$ is asymptotically stable at the equilibrium point if $K_p < -a$ and $K_d < 1$.

3.2 Case with delays ($\tau > 0$)

When $\tau > 0$, by substituting $S = \mathrm{i}\omega$ ($\omega > 0$) into (10), Eq. (10) becomes

$$-K_p - a(\cos\omega\tau - \mathrm{i}\sin\omega\tau) - K_d\omega^{\frac{1}{n}} \left(\cos\frac{\pi}{2n} + \mathrm{i}\sin\frac{\pi}{2n}\right) + \mathrm{i}\omega = 0. \tag{14}$$

Then, separating the real and imaginary parts, Eq. (14) becomes

$$\begin{cases} a\cos\omega\tau = -K_p - K_d\omega^{\frac{1}{n}} \cos\dfrac{\pi}{2n}, \\ a\sin\omega\tau = -\omega + K_d\omega^{\frac{1}{n}} \sin\dfrac{\pi}{2n}. \end{cases} \tag{15}$$

Thus,

$$\omega^2 - 2K_d\omega^{\frac{1}{n}+1}\sin\frac{\pi}{2n} + K_d^2\omega^{\frac{2}{n}} + 2K_pK_d\omega^{\frac{1}{n}}\cos\frac{\pi}{2n} + K_p^2 - a^2 = 0. \tag{16}$$

Let $z = \omega^{\frac{1}{n}}$. Then, Eq. (16) becomes

$$z^{2n} - 2K_d\sin\frac{\pi}{2n}z^{n+1} + K_d^2z^2 + 2K_pK_d\cos\frac{\pi}{2n}z + K_p^2 - a^2 = 0. \tag{17}$$

Lemma 2. (1) If $K_p < a$ and $K_d < 0$, Eq. (17) has no positive roots. (2) If $a < K_p < -a$ and $K_d < 0$, Eq. (17) has only one positive root.

Proof. We define a function $b(z)$ as follows:

$$b(z) = z^{2n} - 2K_d \sin\frac{\pi}{2n} z^{n+1} + K_d^2 z^2 + 2K_p K_d \cos\frac{\pi}{2n} z + K_p^2 - a^2.$$

It then follows that

$$b'(z) = 2nz^{2n-1} - 2K_d(n+1)\sin\frac{\pi}{2n} z^n + 2K_d^2 z + 2K_p K_d \cos\frac{\pi}{2n},$$

and

$$b''(z) = 2n(2n-1)z^{2n-2} - 2K_d n(n+1)\sin\frac{\pi}{2n} z^{n-1} + 2K_d^2.$$

(1) If $K_p < a < 0$ and $K_d < 0$, we have $b'(z) > 0$ for $z \in [0, +\infty)$, which signifies that $b(z)$ is a monotone increasing function. Together with $b(0) = K_p^2 - a^2 > 0$, Eq. (17) has no positive roots.

(2) If $a < K_p < 0$ and $K_d < 0$, then $b'(z) > 0$ for $z \in [0, +\infty)$, which signifies that $b(z)$ is a monotone increasing function. It should be noted that $b(0) = K_p^2 - a^2 < 0$. Therefore, $b(z)$ has a unique positive zero z_0. This implies that Eq. (17) has only one positive root.

If $0 < K_p < -a$ and $K_d < 0$, then $b(0) < 0$ and $b'(0) < 0$. In addition, $\lim_{z\to\infty} b'(z) = +\infty$ and $b''(z) > 0$ for $z \in [0, +\infty)$. Therefore, $b(z)$ is a concave function for $z \in [0, +\infty)$. This indicates that there exists a minimum point z_e such that $b'(z_e) = 0$. That is to say, $b(z)$ is monotonically decreasing at $(0, z_e)$, and monotonically increasing at $(z_e, +\infty)$. Together with $b(0) < 0$, Eq. (17) has a unique positive root z_0 ($z_0 > z_e$). This ends the proof.

Let $\omega_{02} = z_0^n$. Note that $h'(z_0) > 0$. It follows from (15) that

$$\tau_{02} = \frac{1}{\omega_{02}} \arccos\left(\frac{-K_p K_d \omega_{02}^{\frac{1}{n}} \cos\frac{\pi}{2n}}{a}\right). \tag{18}$$

Remark 3. It follows from (16) that $K_p^2 + (1 - 2K_d + K_d^2)\omega^2 - a^2 = 0$ when $n = 1$. Thus, $\omega_{01} = \frac{\sqrt{a^2 - K_p^2}}{|1 - K_d|}$ and $\tau_{01} = \frac{1}{\omega_{01}} \arccos(\frac{-K_p}{a})$ for $n = 1$.

Lemma 3. Suppose that $a < K_p < -a$ and $K_d < 0$. Let $S(\tau) = \mu(\tau) + \mathrm{i}\omega(\tau)$ be the root of (10), given $\mu(\tau_{02}) = 0$ and $\omega(\tau_{02}) = \omega_{02}$. Then the transversality condition can be obtained as follows:

$$\mathrm{Re}\left[\frac{\mathrm{d}S(\tau)}{\mathrm{d}\tau}\right]^{-1}_{\substack{\omega=\omega_{02}\\ \tau=\tau_{02}}} > 0.$$

Proof. Differentiating (10) on both sides with respect to τ, we can obtain

$$\left[\frac{\mathrm{d}S(\tau)}{\mathrm{d}\tau}\right]^{-1} = \frac{(\frac{K_d}{n} S^{\frac{1}{n}} - S)\mathrm{e}^{S\tau}}{aS^2}. \tag{19}$$

Then, we have

$$\begin{aligned}
\mathrm{Re}\left[\frac{\mathrm{d}S(\tau)}{\mathrm{d}\tau}\right]^{-1}_{\substack{\omega=\omega_{02}\\ \tau=\tau_{02}}} &= \frac{-\frac{K_d K_p}{n}\omega_{02}^{\frac{1}{n}} \cos\frac{\pi}{2n} - \frac{K_d^2}{n}\omega_{02}^{\frac{2}{n}} + 2\frac{K_d}{n}\omega_{02}^{\frac{1+n}{n}} \sin\frac{\pi}{2n} - \omega_{02}^2}{-a^2\omega_{02}^2},\\
&= \frac{-\frac{K_d K_p}{n} z_0 \cos\frac{\pi}{2n} - \frac{K_d^2}{n} z_0^2 + 2\frac{K_d}{n} z_0^{n+1} \sin\frac{\pi}{2n} - z_0^{2n}}{-a^2 z_0^{2n}},\\
&= \frac{h'(z_0)}{2na^2 z_0^{2n}}.
\end{aligned} \tag{20}$$

It should be noticed that $h'(z_0) > 0$. Thus, $\mathrm{Re}[\frac{\mathrm{d}S(\tau)}{\mathrm{d}\tau}]^{-1}_{\substack{\omega=\omega_{02}\\ \tau=\tau_{02}}} > 0$, namely, $\mathrm{Re}[\frac{\mathrm{d}S(\tau)}{\mathrm{d}\tau}]_{\substack{\omega=\omega_{02}\\ \tau=\tau_{02}}} > 0$. This ends the proof.

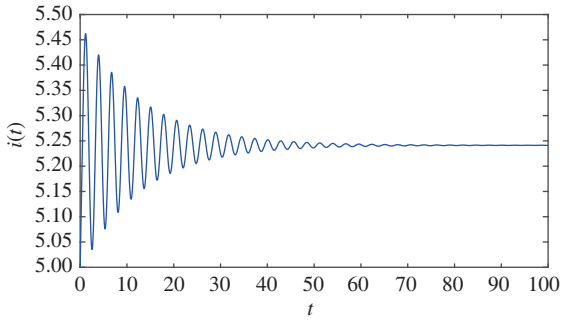

Figure 1 (Color online) Waveform plot of model (2) with initial values $i(0) = 0$, $\varepsilon = 3$, $\mu = 0.1$, and $K_p = K_d = 0$. Model (2) is asymptotically stable at $i^* = 5.241$ when $\tau = 0.69 < \tau_{00}$.

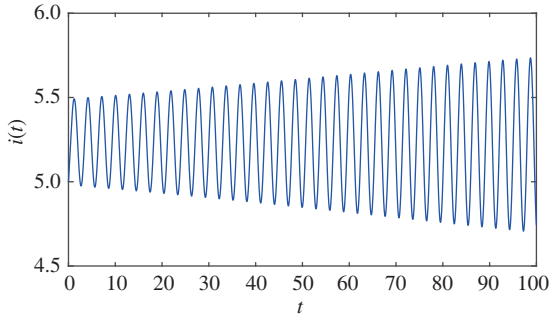

Figure 2 (Color online) Waveform plot of model (2) with initial values $i(0) = 0$, $\varepsilon = 3$, $\mu = 0.1$, and $K_p = K_d = 0$. A Hopf bifurcation occurs when $\tau = 0.75 > \tau_{00}$.

Remark 4. By simple calculation, it is evident that $\mathrm{Re}[\frac{\mathrm{d}S(\tau)}{\mathrm{d}\tau}]^{-1}_{\substack{\omega=\omega_{01}\\ \tau=\tau_{01}}} = \frac{(K_d-1)^2}{a^2} > 0$ when $n = 1$. Therefore, the transversality condition also holds for $n = 1$.

The following results are obtained based on Theorem 2, and Lemmas 2 and 3.

Theorem 3. For the controlled model (5) with $n \in Z^+$ and $\tau > 0$, the following results hold.

(1) If $K_p < a$ and $K_d < 0$, the controlled model (5) is asymptotically stable for $\tau > 0$ at the equilibrium point $i^* = \frac{1+\sqrt{1+4\mu\varepsilon^2}}{2\mu\varepsilon}$.

(2) If $a < K_p < -a$ and $K_d < 0$, the controlled model (5) is asymptotically stable for $\tau \in (0, \tau_{02})$. However, it undergoes a Hopf bifurcation at the equilibrium point $i^* = \frac{1+\sqrt{1+4\mu\varepsilon^2}}{2\mu\varepsilon}$ when $\tau = \tau_{02}$.

Remark 5. When $K_p = 0$ and $K_d = 0$, the conditions in conclusion (2) in Theorem 3 are satisfied for the uncontrolled model (2).

4 Numerical simulation

In this section, we present several examples to demonstrate the aforementioned theories and introduce the effect of the $\mathrm{PD}^{1/n}$ controller. In numerical simulations, we use the predictor-corrector scheme introduced in [39] to determine the solution of delayed fractional-order differential equations. For the sake of comparison, we consider models with the same parameters $\varepsilon = 3$ and $\mu = 0.1$ used in [4, 13]. Therefore, model (2) has a unique equilibrium $i^* = 5.241$.

4.1 Without $\mathrm{PD}^{1/n}$ controller

Eq. (2) becomes

$$\dot{i}(t) = -0.3i^2(t-\tau) + i(t-\tau) + 3.$$

From [40], we can calculate $\tau_{00} = 0.74$. Model (2) is locally asymptotically stable at the equilibrium point when $\tau = 0.69 < \tau_{00}$, which is displayed in Figure 1. In addition, it undergoes a Hopf bifurcation when $\tau = 0.75 > \tau_{00}$, which is illustrated in Figure 2. The corresponding bifurcation diagram is presented in Figure 3. This implies that the bifurcation point obtained by theoretical analysis in [40] is very precise and effective.

4.2 With $\mathrm{PD}^{1/n}$ controller

Next, we apply the $\mathrm{PD}^{1/n}$ controller to the uncontrolled model (2). By changing the control parameters K_p and K_d, we can advance or defer the Hopf bifurcation point of the controlled system. That is, we can optimize the bifurcation characteristics by $\mathrm{PD}^{1/n}$ control.

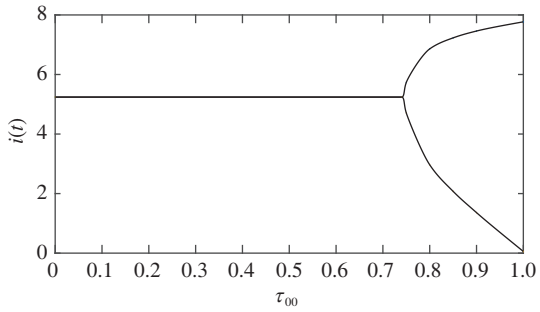

Figure 3 Bifurcation diagram of $i(t)$ vs. τ_{00} with initial values $n = 1$, $i(0) = 0$, $\varepsilon = 3$, $\mu = 0.1$, $K_p = 0.8$, and $K_d = -0.1$.

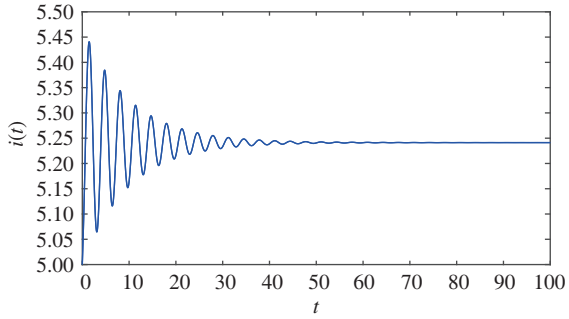

Figure 4 (Color online) Waveform plot of controlled model (5) with initial values $n = 1$, $i(0) = 0$, $\varepsilon = 3$, $\mu = 0.1$, $K_p = 0.8$, and $K_d = -0.1$. Model (5) is asymptotically stable at $i^* = 5.241$ when $\tau = 0.62 < \tau_{01}$.

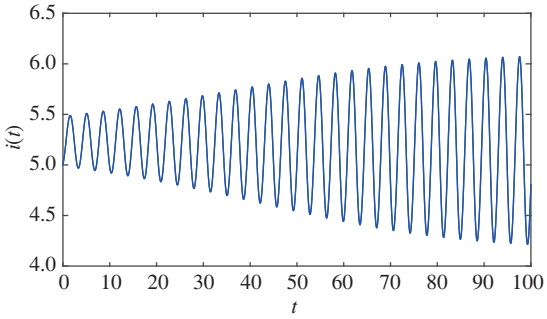

Figure 5 (Color online) Waveform plot of controlled model (5) with initial values $n = 1$, $i(0) = 0$, $\varepsilon = 3$, $\mu = 0.1$, $K_p = 0.8$, and $K_d = -0.1$. A Hopf bifurcation occurs when $\tau = 0.68 > \tau_{01}$.

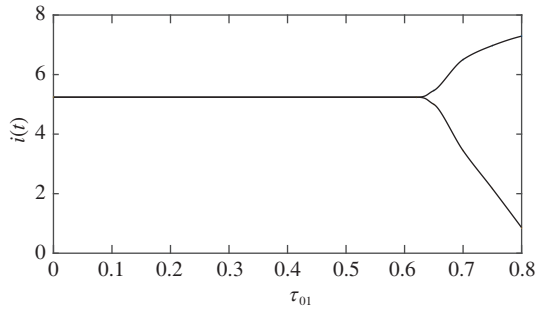

Figure 6 Bifurcation diagram of $i(t)$ vs. τ_{01} with initial values $n = 1$, $i(0) = 0$, $\varepsilon = 3$, $\mu = 0.1$, $K_p = 0.8$, and $K_d = -0.1$.

Example 1 (Under integral-order PD controller ($n = 1$)). (I) We consider $n = 1$, and set $K_p = 0.8$ and $K_d = -0.1$. By Remark 3, we can obtain $\tau_{01} = 0.65$. It can be seen that the critical value $\tau_{01} = 0.65$ of the controlled model (5) is smaller than $\tau_{00} = 0.74$ of the original congestion model (2). This signifies that the critical value is advanced with the integral-order PD controller with $K_p = 0.8$ and $K_d = -0.1$. According to Theorem 2, the controlled model (5) is locally asymptotically stable at the equilibrium point when $\tau = 0.62 < \tau_{01}$, as illustrated in Figure 4. In addition, a Hopf bifurcation occurs when $\tau = 0.68 > \tau_{01}$, as displayed in Figure 5. The corresponding bifurcation diagram is presented in Figure 6.

(II) We set $n = 1$, $K_p = 0.7$, and $K_d = -0.5$. It follows from Remark 3 that $\tau_{01} = 0.92$, which is larger than $\tau_{00} = 0.74$ of model (2). This indicates that the Hopf bifurcation point is delayed by the designed PD controller with $K_p = 0.7$ and $K_d = -0.5$. From Theorem 2, model (5) is asymptotically stable at $i^* = 5.241$ for $\tau \in [0, \tau_{01})$, and unstable when $\tau > \tau_{01}$. Figure 7 displays the trend of model (5) when $\tau = 0.88 < \tau_{01}$, while Figure 8 illustrates the periodic oscillation when $\tau = 0.94 > \tau_{01}$. The corresponding bifurcation diagram is presented in Figure 9.

Example 2 (Under fractional-order PD$^{1/n}$ controller ($n > 1$)). (I) To advance the bifurcation of model

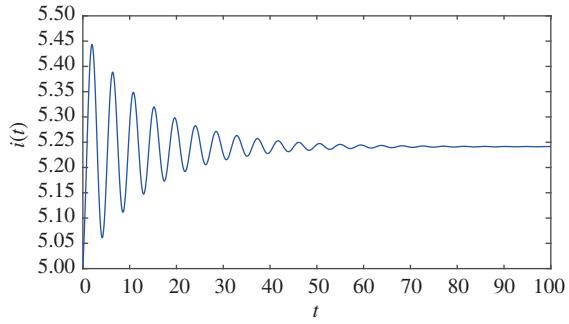

Figure 7 (Color online) Waveform plot of controlled model (5) with initial values $n = 1$, $i(0) = 0$, $\varepsilon = 3$, $\mu = 0.1$, $K_p = 0.7$, and $K_d = -0.5$. Model (5) is asymptotically stable at $i^* = 5.241$ when $\tau = 0.88 < \tau_{01}$.

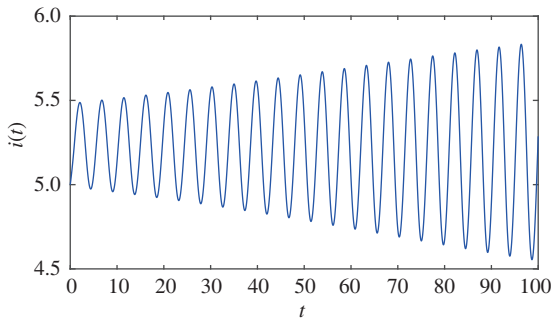

Figure 8 (Color online) Waveform plot of controlled model (5) with initial values $n = 1$, $i(0) = 0$, $\varepsilon = 3$, $\mu = 0.1$, $K_p = 0.7$, and $K_d = -0.5$. A Hopf bifurcation occurs when $\tau = 0.94 > \tau_{01}$.

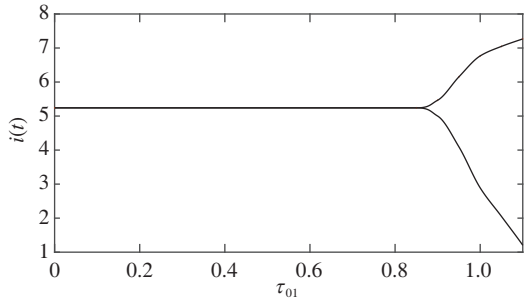

Figure 9 Bifurcation diagram of $i(t)$ vs. τ_{01} with initial values $n = 1$, $i(0) = 0$, $\varepsilon = 3$, $\mu = 0.1$, $K_p = 0.7$, and $K_d = -0.5$.

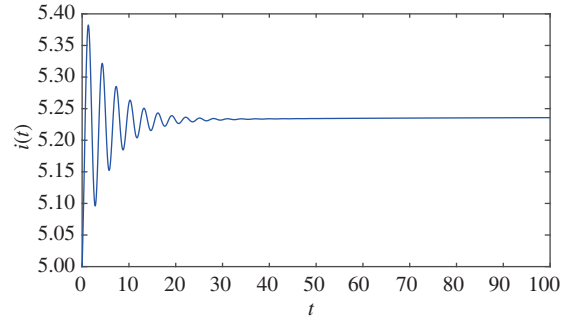

Figure 10 (Color online) Waveform plot of controlled model (5) with initial values $n = 3$, $i(0) = 0$, $\varepsilon = 3$, $\mu = 0.1$, $K_p = 0.8$, and $K_d = -0.2$. Model (5) is asymptotically stable at $i^* = 5.241$ when $\tau = 0.60 < \tau_{02}$.

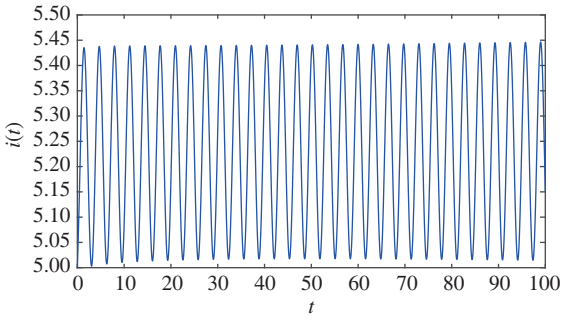

Figure 11 (Color online) Waveform plot of controlled model (5) with initial values $n = 3$, $i(0) = 0$, $\varepsilon = 3$, $\mu = 0.1$, $K_p = 0.8$, and $K_d = -0.2$. The equilibrium is unstable when $\tau = 0.68 > \tau_{02}$.

(2), we select $n = 3$, $K_p = 0.8$ and $K_d = -0.2$. By (18), we obtain $\tau_{02} = 0.65$. From Theorem 3, model (5) is asymptotically stable at $i^* = 5.241$ for $\tau \in [0, \tau_{02})$, and unstable when $\tau > \tau_{02}$. Figure 10 displays that the controlled model (5) is stable when $\tau = 0.60 < \tau_{02}$. A periodic oscillation occurs through a Hopf bifurcation when $\tau = 0.68 > \tau_{02}$, as illustrated in Figure 11. It should be noted that $\tau_{02} = 0.65 < \tau_{00} = 0.74$. That is, the critical point of the system is advanced. The corresponding bifurcation diagram is presented in Figure 12.

(II) Next, we select $K_p = -0.2$, $K_d = -0.2$ and $n = 3$ to delay the Hopf bifurcation. By (18), we obtain $\tau_{02} = 0.89$. From Theorem 3, the controlled model (5) is asymptotically stable for $\tau \in [0, \tau_{02})$, and unstable when $\tau > \tau_{02}$. The experimental research on different numbers for the delay are graphically displayed in Figures 13 and 14. The corresponding bifurcation diagram is presented in Figure 15.

It should be noted that the fractional-order PD controller degenerates to an integer-order controller

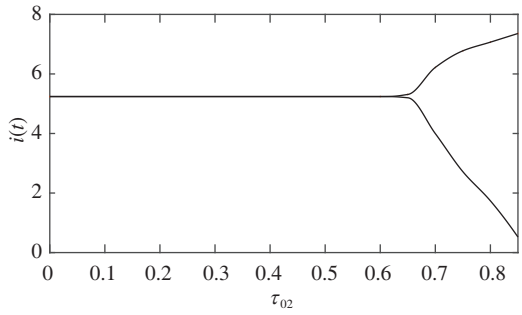

Figure 12 Bifurcation diagram of $i(t)$ vs. τ_{02} with initial values $n = 3$, $i(0) = 0$, $\varepsilon = 3$, $\mu = 0.1$, $K_p = 0.8$, and $K_d = -0.2$.

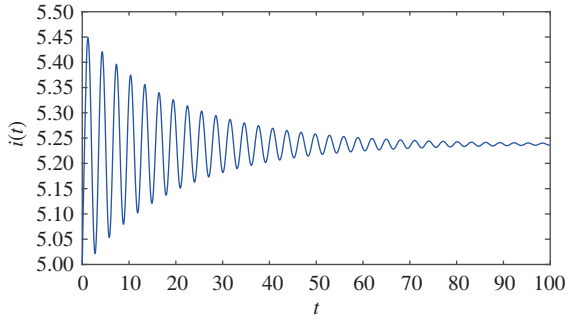

Figure 13 (Color online) Waveform plot of controlled model (5) with initial values $n = 3$, $i(0) = 0$, $\varepsilon = 3$, $\mu = 0.1$, $K_p = -0.2$, and $K_d = -0.2$. The equilibrium is asymptotically stable when $\tau = 0.87 < \tau_{02}$.

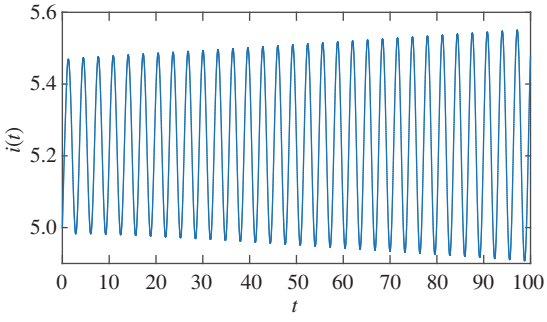

Figure 14 (Color online) Waveform plot of controlled model (5) with initial values $n = 3$, $i(0) = 0$, $\varepsilon = 3$, $\mu = 0.1$, $K_p = -0.2$, and $K_d = -0.2$. The equilibrium is unstable at $i^* = 5.241$ when $\tau = 0.91 > \tau_{02}$.

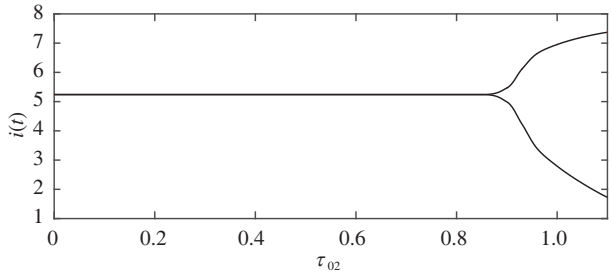

Figure 15 Bifurcation diagram of $i(t)$ vs. τ_{02} with initial values $n = 3$, $i(0) = 0$, $\varepsilon = 3$, $\mu = 0.1$, $K_p = -0.2$, and $K_d = -0.2$.

($n = 1$), and Example 1 demonstrates that the critical value of Hopf bifurcations can be both delayed and advanced when an integer-order PD controller is used. Example 2 draws another contrast; when the fractional-order PD controller ($n > 1$) is applied, we can also manipulate the bifurcation point by altering the control gain parameters K_p and K_d.

4.3 Influence of K_p, K_d, and n on critical value τ_0

In this subsection, we discuss the influence of the control gain parameters K_p, K_d, and n on the critical value τ_0. First, we examine the effect of K_d on τ_0 with fixed K_p. Figure 16 depicts the relationship of K_d and τ_0 with $K_p = -0.5$. We conclude that the values of τ_0 decline with an increase in K_d. In addition, the descending speed of τ_0 becomes increasingly clear with an increase in n. Figure 17 illustrates the relationship of K_p and τ_0 with $K_p = -2$. Similarly, the value of τ_0 decreases with an increase in K_p and the rate of descent decreases with an increase in n.

According to the above analysis, we can determine that n also has a large influence on the change of

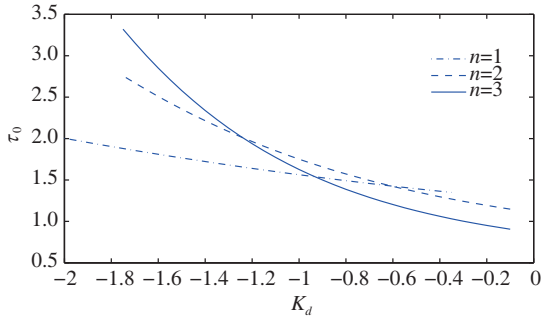

Figure 16 (Color online) Relationship between K_d and τ_0 with fixed $K_p = -0.5$.

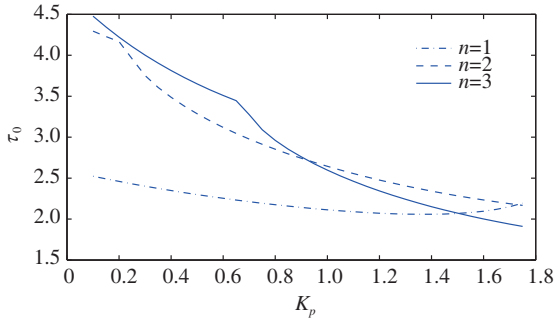

Figure 17 (Color online) Relationship between K_p and τ_0 with fixed $K_d = -2$.

Table 1 Effect of n on value of τ_0 for controlled system (5) with $K_p = -1$ and $K_d = -1$

Fractional-order parameter n	Bifurcation point τ_0
1	0.8855
2	0.7856
3	0.7761
4	0.7735
5	0.7720
6	0.7711
7	0.7706
8	0.7703

the bifurcation point τ_0. Table 1 illustrates the influence of n on the bifurcation point τ_0 when $K_p = -1$, $K_d = -1$, $\varepsilon = 3$, and $\mu = 0.1$. Disregarding the integer-order case ($n = 1$), we can draw the conclusion that the bifurcation point τ_0 monotonically decreases with an increase in n ($n \geqslant 2$). In addition, Table 1 indicates that the controlled small-world network model is difficult to keep stable with a larger delay, and it is more likely to have a Hopf bifurcation as the delay τ increases.

As seen in Table 1, changing n from 1 to 8 results in the monotonic decreasing of τ_0. Therefore, τ_0 has a maximum value when $n = 1$.

5 Conclusion

In this study, a fractional-order $\mathrm{PD}^{1/n}$ controller is designed for the first time and applied to an integer-order small-world model. The results demonstrate that the designed PD controller can be used to restrain or promote the occurrence of Hopf bifurcations by setting appropriate parameters. In addition, the stability and Hopf bifurcation conditions of the controlled model with a fractional-order PD controller are obtained.

In future work, we will focus on a more general fractional-order controller. In addition, we will study the influence of the controller on the dynamics of the controlled system. To improve the dynamic performance of the system, we will apply the designed controller to more general real systems.

Acknowledgements This work was supported in part by National Natural Science Foundation of China (Grant Nos. 61573194, 51775284, 61877033), Natural Science Foundation of Jiangsu Province of China (Grant Nos. BK20181389, BK20181387), Key Project of Philosophy and Social Science Research in Colleges and Universities in Jiangsu Province (Grant No. 2018SJZDI142), and Postgraduate Research & Practice Innovation Program of Jiangsu Province (Grant No. KYCX18_0924).

References

1 Watts D J, Strogatz S H. Collective dynamics of 'small-world' networks. Nature, 1998, 393: 440–442

2 Newman M E J, Watts D J. Renormalization group analysis of the small-world network model. Phys Lett A, 1999, 263: 341–346
3 Yang X S. Chaos in small-world networks. Phys Rev E, 2001, 63: 046206
4 Xiao M, Ho D W C, Cao J D. Time-delayed feedback control of dynamical small-world networks at Hopf bifurcation. Nonlinear Dyn, 2009, 58: 319–344
5 Xu X, Luo J W. Dynamical model and control of a small-world network with memory. Nonlinear Dyn, 2013, 73: 1659–1669
6 Li C G, Chen G R. Local stability and Hopf bifurcation in small-world delayed networks. Chaos Solitons Fract, 2004, 20: 353–361
7 Li N, Sun H Y, Zhang Q L. Bifurcations and chaos control in discrete small-world networks. Chin Phys B, 2012, 21: 010503
8 Liu F, Guan Z H, Wang H. Controlling bifurcations and chaos in discrete small-world networks. Chin Phys B, 2008, 17: 2405–2411
9 Mahajan A V, Gade P M. Transition from clustered state to spatiotemporal chaos in a small-world networks. Phys Rev E, 2010, 81: 056211
10 Wu X Q, Zhao X Y, Lü J H, et al. Identifying topologies of complex dynamical networks with stochastic perturbations. IEEE Trans Control Netw Syst, 2016, 3: 379–389
11 Maslennikov O V, Nekorkin V I, Kurths J. Basin stability for burst synchronization in small-world networks of chaotic slow-fast oscillators. Phys Rev E, 2015, 92: 042803
12 Mei G F, Wu X Q, Ning D, et al. Finite-time stabilization of complex dynamical networks via optimal control. Complexity, 2016, 21: 417–425
13 Xiao M, Zheng W X, Lin J X, et al. Fractional-order PD control at Hopf bifurcations in delayed fractional-order small-world networks. J Franklin Inst, 2017, 354: 7643–7667
14 Zhou J, Xu X, Yu D Y, et al. Stability, instability and bifurcation modes of a delayed small world network with excitatory or inhibitory short-cuts. Int J Bifurcat Chaos, 2016, 26: 1650070
15 Cao J D, Guerrini L, Cheng Z S. Stability and Hopf bifurcation of controlled complex networks model with two delays. Appl Math Comput, 2019, 343: 21–29
16 Cao Y. Bifurcations in an Internet congestion control system with distributed delay. Appl Math Comput, 2019, 347: 54–63
17 Hassard B D, Kazarinoff N D, Wan Y H. Theory and Applications of Hopf bifurcation. Cambridge: Cambridge University Press, 1981
18 Han M A, Sheng L J, Zhang X. Bifurcation theory for finitely smooth planar autonomous differential systems. J Differ Equ, 2018, 264: 3596–3618
19 Tian H H, Han M A. Bifurcation of periodic orbits by perturbing high-dimensional piecewise smooth integrable systems. J Differ Equ, 2017, 263: 7448–7474
20 Liu L S, Sun F L, Zhang X G. Bifurcation analysis for a singular differential system with two parameters via to topological degree theory. Nonlinear Anal Model Control, 2017, 22: 31–50
21 Li S Q, Peng X Y, Tang Y, et al. Finite-time synchronization of time-delayed neural networks with unknown parameters via adaptive control. Neurocomputing, 2018, 308: 65–74
22 Guo W C, Yang J D. Hopf bifurcation control of hydro-turbine governing system with sloping ceiling tailrace tunnel using nonlinear state feedback. Chaos Soliton Fract, 2017, 104: 426–434
23 Ali M S, Yogambigai J. Passivity-based synchronization of stochastic switched complex dynamical networks with additive time-varying delays via impulsive control. Neurocomputing, 2018, 273: 209–221
24 Liu R J, She J H, Wu M, et al. Robust disturbance rejection for a fractional-order system based on equivalent-input-disturbance approach. Sci China Inf Sci, 2018, 61: 070222
25 Al Hosani K, Nguyen T H, Al Sayari N. Fault-tolerant control of MMCs based on SCDSMs in HVDC systems during DC-cable short circuits. Int J Electr Power Energ Syst, 2018, 100: 379–390
26 Ding D W, Zhang X Y, Cao J D, et al. Bifurcation control of complex networks model via PD controller. Neurocomputing, 2016, 175: 1–9
27 Tang Y H, Xiao M, Jiang G P, et al. Fractional-order PD control at Hopf bifurcations in a fractional-order congestion control system. Nonlinear Dyn, 2017, 90: 2185–2198
28 Zhang W Z, Dong X K, Liu X Y. Switched fuzzy-PD control of contact forces in robotic microbiomanipulation. IEEE Trans Biomed Eng, 2017, 64: 1169–1177
29 Ouyang P R, Pano V, Tang J, et al. Position domain nonlinear PD control for contour tracking of robotic manipulator. Robot Comput-Integr Manuf, 2018, 51: 14–24
30 Özbay H, Bonnet C, Fioravanti A R. PID controller design for fractional-order systems with time delays. Syst Control

Lett, 2012, 61: 18–23
31 Wu J, Zhang X G, Liu L S, et al. Iterative algorithm and estimation of solution for a fractional order differential equation. Bound Value Probl, 2016, 2016: 116
32 Li M M, Wang J R. Exploring delayed Mittag-Leffler type matrix functions to study finite time stability of fractional delay differential equations. Appl Math Comput, 2018, 324: 254–265
33 Zhang X G, Liu L S, Wu Y H. The uniqueness of positive solution for a fractional order model of turbulent flow in a porous medium. Appl Math Lett, 2014, 37: 26–33
34 Bao F X, Yao X X, Sun Q H, et al. Smooth fractal surfaces derived from bicubic rational fractal interpolation functions. Sci China Inf Sci, 2018, 61: 099104
35 Guan Y L, Zhao Z Q, Lin X L. On the existence of positive solutions and negative solutions of singular fractional differential equations via global bifurcation techniques. Bound Value Probl, 2016, 2016: 141
36 Shao J, Zheng Z W, Meng F W. Oscillation criteria for fractional differential equations with mixed nonlinearities. Adv Differ Equ, 2013, 2013: 323
37 Podlubny I. Fractional Differential Equations. New York: Academic Press, 1999
38 Li C P, Deng W H. Remarks on fractional derivatives. Appl Math Comput, 2007, 187: 777–784
39 Bhalekar S, Varsha D. A predictor-corrector scheme for solving nonlinear delay differential equations of fractional order. J Fractional Calc Appl, 2011, 1: 1–9
40 Zhang C, Zhao D H, Ruan J. Delay induced Hopf bifurcation of small-world networks. Chin Ann Math Ser B, 2007, 28: 453–462